



Radiation Shielding Study of Heavy Metal Oxide Bismuth-Tungsten Borate Based Glasses for Defense and Medical Applications

Muhammad Fakhrul Naim Jaafar¹, Bashar Khudhair Abbas², Sharudin Omar Baki^{3*}, Yaakob Mansor³, Muhammad Khalis Abdul Karim¹, Mohd Adzir Mahdi⁴

¹ Department of Physics, Faculty of Science, Universiti Putra Malaysia, 43400 Serdang, Selangor, Malaysia

² Dept. Medical Inst. Engineering, Al Hikma University College, Baghdad, Iraq

³ Physics Division, Centre of Foundation Studies for Agricultural Science, Universiti Putra Malaysia, 43400 Serdang, Selangor, Malaysia

⁴ Wireless and Photonic Network Research Centre, Faculty of Engineering, Universiti Putra Malaysia, 43400 Serdang, Selangor, Malaysia

ABSTRACT

In this work, series of bismuth-tungsten-borate oxide glasses: $(90-x)\text{B}_2\text{O}_3-10\text{WO}_3-x\text{Bi}_2\text{O}_3$, $x=5, 10, 15, 20, 25$, were produced using conventional high temperature melt-quenching method. The obtained glasses show reduction in opacity and become denser as bismuth concentration increases. The molar volume also increases which may explain due to structural deformation of the glass matrix by the bismuth atoms once its concentration increases. In order to understand the bismuth effect on radiation shielding, we investigated the physical and ionizing shielding characteristics within energy range of 0.015 until 15 MeV. The mass attenuation coefficient (MAC), Half-Value-Layer (HVL) and Mean-Free-Path (MFP) parameters were fully explored throughout the study for photon shielding and advanced defense and medical applications.

Keywords:

Glass; melt-quenching; heavy metal oxide; radiation shielding; mass attenuation coefficient

1. Introduction

Heavy metal oxide (HMO) recently has greatly increased interest among radiation shielding researchers due to its potential as shielding materials. Various HMOs have been incorporated into the glass matrices such as bismuth (Bi_2O_3), lead (PbO), strontium (SrO), tungsten (WO_3) and lanthanide series oxide elements [1-4]. As these oxides known to have higher density and acted as active glass modifier, they are promising to enhance the shielding ability of the shielding glasses. Borate (B_2O_3) glasses consisting of bismuth have shown an excellent radiation shielding candidate due its massive nature with higher density, refractive index, optical susceptibility and high polarizability. As compared to lead, bismuth is non-toxic with high radiation shielding behavior and moisture resistance [5].

Furthermore, borate as glass former is well associated with bismuth ion which acted as network modifier where it reduces the crystallization rate of glass formation [6]. Borate glasses itself are

* Corresponding author.

E-mail address: sharudinomar@upm.edu.my

<https://doi.org/10.37934/araset.61.2.268275>

known solely a good glass former with good thermal stability and low melting point in which its smaller cation size moderate volume occupancy for large glass forming ability for bismuth and rare-earth ions in radiation shielding and optical applications. WO_3 , is also considered as potential HMO and known recently as an important element for smart glass called electrochromic windows [7]. WO_3 also possesses high density structure of 19.3 g/cm^3 comparatively among most metals which would act as an excellent glass modifier once incorporated in glass. As glass nature is known with its transparency to visible light and lighter as compared to conventional metal and concrete structure, we strongly believe the incorporation of tungsten will strengthen the designed glass system and enhances the shielding properties by minimizing the hazardous of radiation such as x-rays and gamma rays especially in critical safety issue such in medical and military operation procedure.

2. Methodology

2.1 Sample Fabrication

Melt quenching method at high melting temperature was performed to produce ternary B_2O_3 - WO_3 - Bi_2O_3 glass samples. Five batches sample series were carefully weighed via electronic balance for each 10 g mixture consisting: $(90-x)B_2O_3$ - $10WO_3$ - xBi_2O_3 , $x= 5, 10, 15, 20, 25$ mole percentage (with purity of more than 90%). Alumina crucible was used to melt the composition up to 1100°C in an automatic control electrical furnace for an hour. Finally, the molten glass was quickly poured onto casting steel mould and allowed to cool slowly to room temperature. Then all the glass samples were annealed at 300°C for an hour to avoid cracking due thermal internal stress. The fabricated series samples are shown in Figure 1, whereas observed the transparency reduce as bismuth content increases.



Fig. 1. Series of B_2O_3 - WO_3 - Bi_2O_3 glass samples fabricated

2.2 Density and Molar Volume Measurement

All the glass samples density was obtained by using electronic Alfa Mirage MD-300S densimeter with $\pm 0.001 \text{ g/cm}^3$ accuracy. In general Archimedes' Principle [8] using water as medium, the density of the sample ρ , is determined using,

$$\rho = \frac{W_{air}}{W_{air}-W_{water}} \times \rho_{water} \quad (1)$$

where W_{air} , is the sample weight in air, W_{water} is the sample weight in water and ρ_{water} is the density of water ($\rho_{water} = 0.998 \text{ g/cm}^3$). Using the measured glass density, the molar volume (V_M) can be calculated [9] from:

$$V_M = \frac{M_w}{\rho} \quad (2)$$

where M_w is molecular weight of the glass samples. This quantity is defined by the volume occupied by a mole of glass formulation which will further explain the compactness and bonding nature of the glass.

2.3 Radiation Shielding Measurement

In this work the radiation shielding parameters for all samples by photon energies ranges from 0.015 MeV up to 15 MeV, namely as mass attenuation coefficient (MAC), half-value layer (HVL) and mean free path (MFP) were determine through simulation via Phy-X/PSD software [10]. If a photon from gamma-ray penetrates the glass sample of thickness x , its initial intensity I_0 will be attenuated following the Lambert-Beer law [11] as given below:

$$I = I_0 e^{-\mu x} \quad (3)$$

where I and μ is the beam intensity after passing through the sample and linear attenuation coefficient respectively. Using the above Lambert-Beer law, MAC is defined by the ratio of the linear attenuation coefficient to sample density as [12]:

$$MAC = \frac{1}{\rho x} \ln \frac{I_0}{I} \quad (4)$$

This quantity is characterized the ability of photon energy penetrate through a given mass, which also means absorption cross section of the materials. Since the glass samples consist of multi-composition oxides, total MAC will be the summation of each MAC of the constituent oxides (for ternary glass where 3 oxides compositions) using mixing rule [13]:

$$MAC_{sample} = \sum_{i=1}^3 w_i MAC_i \quad (5)$$

where w_i and MAC_i referring to the weight percentage of the oxide and its corresponding MAC respectively.

For a given material thickness which attenuated the incident photon rays to one half of its value is define as the half value layer (HVL) [14]. By simply using Eq. (2):

$$HVL = \frac{\ln 2}{\mu} \quad (6)$$

In this case the higher material density the higher the HVL values. The probability of photons interaction within the materials is called mean free path (MFP) [15]. It is referring to average successive photon-photon collision distance and dependent on material density.

$$MFP = \frac{1}{\mu} \quad (7)$$

3. Results

3.1 Density-Molar Volume Relationship

Table 1 shows the density-molar volume values of the S1-S5 samples. As observed and expected replacement of lighter borate content with massive bismuth oxide have increased the density of all glass samples significantly from 4.172 to 4.844 g/cm³ due to density of bismuth (Bi₂O₃ density = 8.90 g/cm³) is three times larger than borate (Bi₂O₃ density = 2.55 g/cm³). It also can be explained by a larger difference in terms of molecular weight between them (M(Bi₂O₃)=465.96 g/mol, M(B₂O₃)=69.61 g/mol). The molar volume also shows similar trend of increment which could be due to bigger atomic size of bismuth (Z=83) as compared to boron atom (Z=5). The substitution of larger bismuth atom has modified and created more open structure within the interstitial of the glass matrix. Kaky *et al.*, [16] reported greater formation of non-bridging oxygen (NBO) have resulted more void spaces of the glass network.

Table 1

Composition and physical properties of the prepared samples

Sample code	Mol percentage (%)			Density, ρ (g/cm ³)	Molar volume, V_m (cm ³ /mol)
	B ₂ O ₃	WO ₃	Bi ₂ O ₃		
S1	85	10	5	4.172	25.325
S2	80	10	10	4.285	29.284
S3	75	10	15	4.400	33.023
S4	70	10	20	4.781	34.535
S5	65	10	25	4.844	38.175

3.2 Gamma Ray Shielding Properties

The obtained mass attenuation coefficients with respect to photon energies within 0.015-15 MeV are as shown in Figure 2. All samples shown similar trends of abrupt reduction in MAC for lower energy region then slowly decrease and reach almost constant at higher energy range. As the energy getting higher, the penetration of the gamma radiation will be also higher into the glass samples, which explained such smaller in MAC. Noticed there is sudden MAC peak at 0.1 MeV which is due to bismuth K-edge absorption [17].

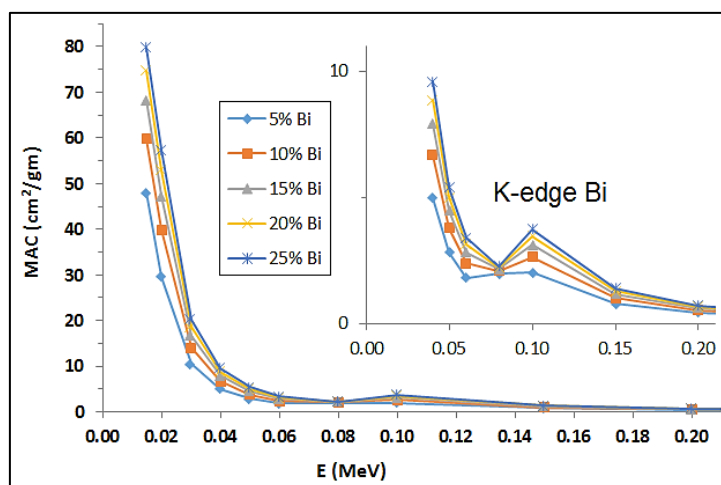


Fig. 2. Mass attenuation coefficients (MAC) within 0.015-15 MeV photon energies

Figures 3(a) and 3(b) presented the variation of MAC with different bismuth content for lower and intermediate photon energies respectively. As one can observed MAC is higher for higher bismuth content samples where sample S5 achieves the highest MAC around 80 cm²/gm at 0.015 MeV, then followed in order by S4>S3>S2>S1. Interaction of photon with materials at lower photon energies is mostly due to photoelectric effect where sharp decrement in MAC occurred, while Compton scattering, and pair production are responsible for intermediate and higher energies range respectively [18,19].

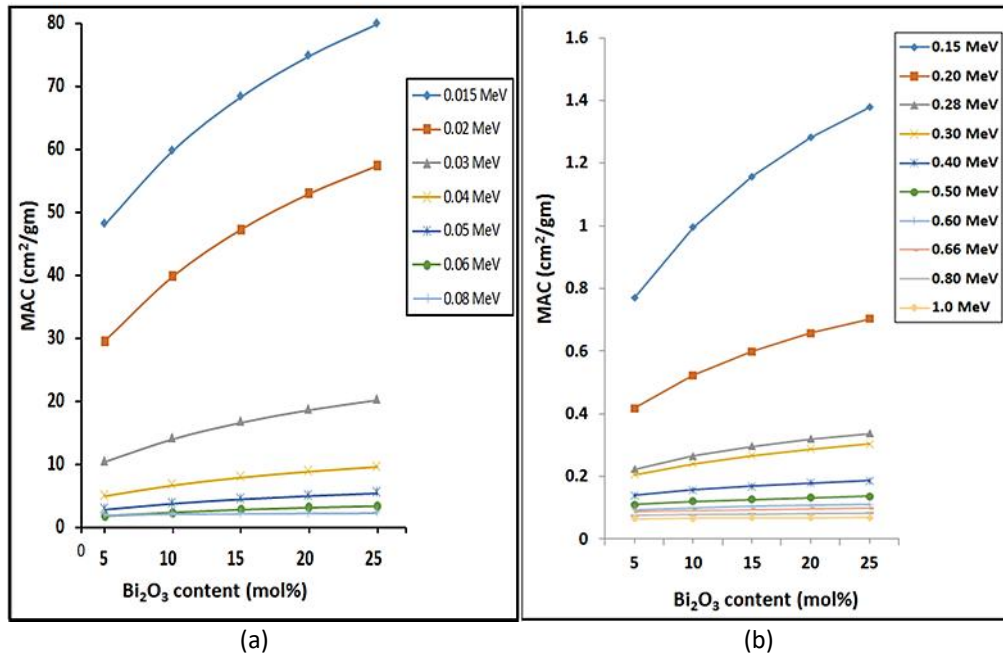


Fig. 3. MAC variation of photon energies (a) Lower (b) Intermediate

It is important to ensure the thickness of the shielding materials be able to attenuate the gamma radiation as much as possible. In this work the HVL represented in Figure 4(a) suggested the required thickness to cut-off 50% of the intensity of incident photon at specific energy. The obtained HVL values increased sharply at lower energies below 1 MeV then gradually increase beyond it. As can be observed the higher the bismuth content the lower the HVL values, indicating S5 glass sample which known with highest MAC previously is effectively attenuated the gamma rays as compared to other samples via utilizing more thinner glass. HVL values for selected incident photon energies at 0.30, 0.662, 1.0 and 1.50 MeV are shown in Figure 4(b) concluded lowest HVL values were obtained by lowest photon energy with higher bismuth content.

Subsequently, our HVL findings are performing much better results for higher gamma energy beyond 1 MeV as shown in Figure 5. The fabricated glass is having better protection as compare to some type of concretes (ordinary, ilmenite and basalt-magnetite) and other borate glasses which does not incorporating any heavy metal oxide [20]. Thus, we are confident the proposed glass composition is highly useful in military and medical field which required transparent visible view operations [20]. The HVL values of the prepared glasses have been compared with three types of concretes (ordinary, ilmenite and basalt-magnetite).

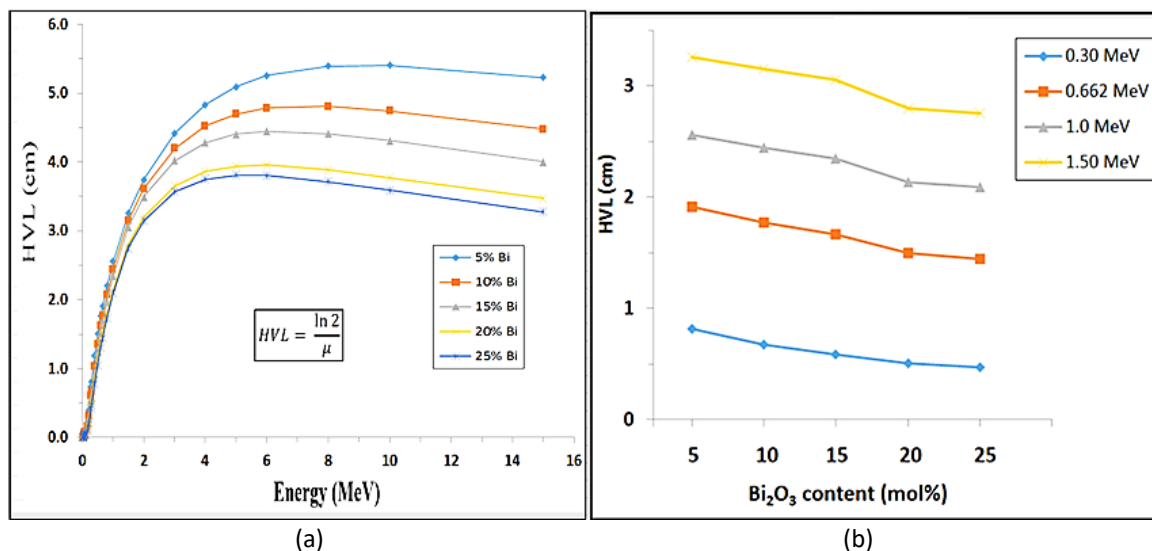


Fig. 4. HVL values for photon energies (a) Within 0.015-15 MeV (b) Specific incident

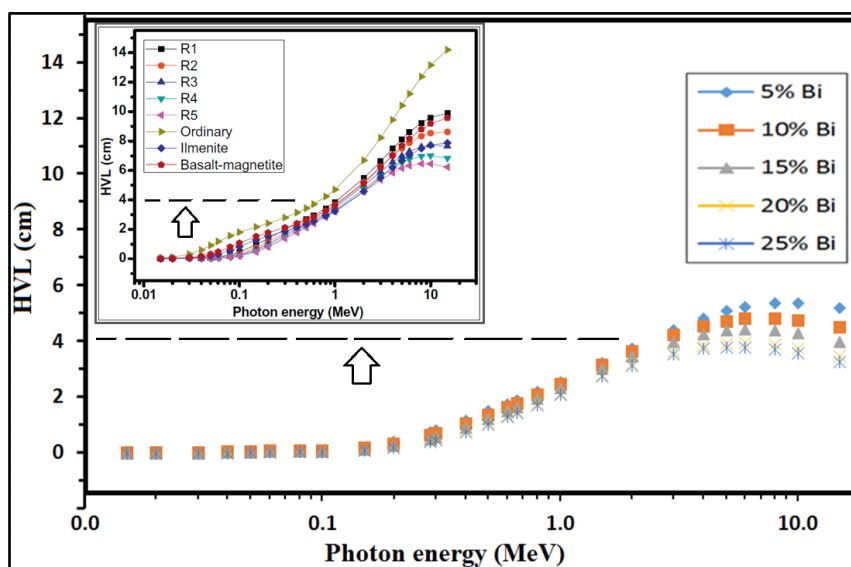


Fig. 5. HVL as compared to some type of concretes and reported glasses (inserted plot as comparison [20])

Figure 6 represented MFP analysis for the five glass samples at selected photon energies. It is obvious in Figure 6(a) the highest MFP value was recorded for highest photon energy when penetrated into the lowest bismuth content glass. As can be seen in Figure 6(b) MFP values are less affected even though the bismuth content increases. Nevertheless, for highest photon energy at 15 MeV, the MFP significantly reduced with the increment of the bismuth content in the glasses. From the radiation shielding perspective the lower MFP value for a given photon energy the better the shielding property.

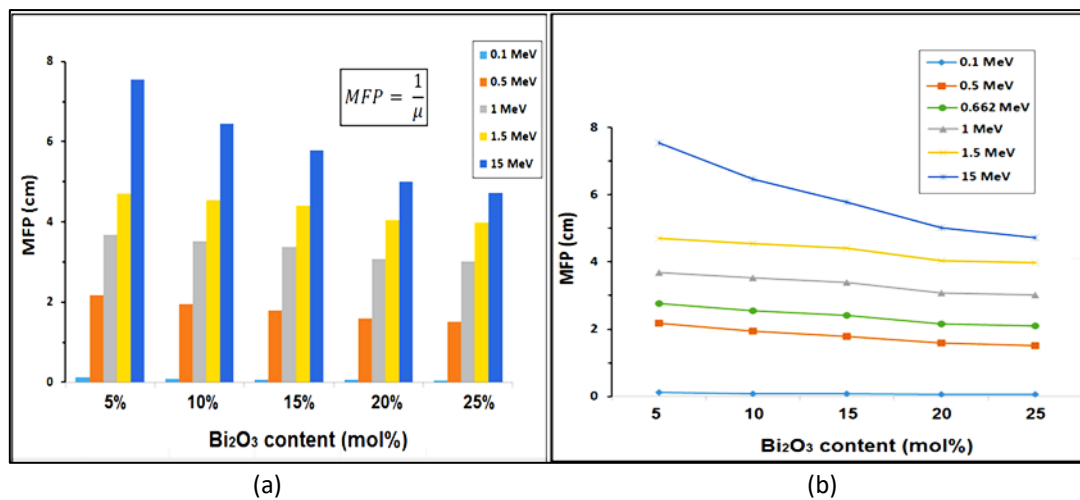


Fig. 6. (a) MFP analysis for the five glass samples at selected photon energies (b) Variation of MFP trends as bismuth content changes

4. Conclusions

We accomplished fabricated ternary B₂O₃-WO₃-Bi₂O₃ glass samples series via high temperature melt-quenching method by modulating bismuth content in HMO borate-based composition. Denser glasses with increment molar volume were produced by incorporation larger bismuth ion into borate glass matrix. Radiation shield parameters MAC, HVL and MFP were analysed comprehensively in order to explore the glasses capability for gamma ray protection. The obtained results shown superior shielding behaviour as bismuth content increasing where sample S5 achieves the highest MAC around 80 cm²/gm at 0.015 MeV with lower HVL values as compared to other shielding materials reported so far. Without doubt the proposed glass system is promising materials for future design gamma shield in both defence and medical applications.

Acknowledgement

This research was funded by Universiti Putra Malaysia (UPM) under Geran Putra Berimpak, (GP-GPB/2021/9707700).

References

- [1] Fong, W. L., Sharudin Omar Baki, N. M. Arifin, Yaakob Mansor, Ahmad Nazri, and Bashar Khudhair Abbas. "Structural, thermal and optical properties of rare earth doped lead tellurite oxide glasses." *Journal of Advanced Research in Fluid Mechanics and Thermal Sciences* 81, no. 2 (2021): 52-58. <https://doi.org/10.37934/arfmts.81.2.5258>
- [2] Bashar, Kh A., G. Lakshminarayana, S. O. Baki, Al-BFA Mohammed, U. Caldiño, A. N. Meza-Rocha, Vijay Singh, I. V. Kityk, and M. A. Mahdi. "Tunable white-light emission from Pr³⁺/Dy³⁺ co-doped B₂O₃-TeO₂ PbO-ZnO Li₂O-Na₂O glasses." *Optical Materials* 88 (2019): 558-569. <https://doi.org/10.1016/j.optmat.2018.12.028>
- [3] Bashar, Kh A., W. L. Fong, Kh A. Haider, S. O. Baki, M. H. M. Zaid, and M. A. Mahdi. "Optical studies on Tb³⁺: Dy³⁺ singly and doubly doped Borosilicate glasses for white light and solid state lighting applications." *Journal of Non-Crystalline Solids* 534 (2020): 119943. <https://doi.org/10.1016/j.noncrysol.2020.119943>
- [4] Zang, X. M., D. S. Li, E. Y. B. Pun, and H. Lin. "Dy 3+ doped borate glasses for laser illumination." *Optical Materials Express* 7, no. 6 (2017): 2040-2054. <https://doi.org/10.1364/OME.7.002040>
- [5] Fong, W. L., Kh A. Bashar, S. O. Baki, M. H. M. Zaid, B. T. Goh, and M. A. Mahdi. "Thermal, structural and optical properties of Bi₂O₃-Na₂O-TiO₂-ZnO-TeO₂ glass system." *Journal of Non-Crystalline Solids* 555 (2021): 120621. <https://doi.org/10.1016/j.noncrysol.2020.120621>
- [6] Fong, W. L., KhA Bashar, S. O. Baki, M. K. A. Karim, M. I. Sayyed, M. A. Mahdi, B. T. Goh, and O. B. Aljewaw. "Influence of Bi₂O₃ content on structural, optical and radiation shielding properties of transparent Bi₂O₃-Na₂O-TiO₂-ZnO-TeO₂

- glass ceramics." *Radiation Physics and Chemistry* 200 (2022): 110289. <https://doi.org/10.1016/j.radphyschem.2022.110289>
- [7] Lakshminarayana, G., S. O. Baki, A. Lira, I. V. Kityk, U. Caldiño, Kawa M. Kaky, and M. A. Mahdi. "Structural, thermal and optical investigations of Dy₃₊-doped B₂O₃-WO₃-ZnO-Li₂O-Na₂O glasses for warm white light emitting applications." *Journal of Luminescence* 186 (2017): 283-300. <https://doi.org/10.1016/j.jlumin.2017.02.049>
- [8] Elkhoshkhany, N., Rafik Abbas, R. El-Mallawany, and S. F. Hathot. "Optical properties and crystallization of bismuth boro-tellurite glasses." *Journal of Non-Crystalline Solids* 476 (2017): 15-24. <https://doi.org/10.1016/j.jnoncrysol.2017.06.031>
- [9] Suthanthirakumar, P., and K. Marimuthu. "Investigations on spectroscopic properties of Dy³⁺ doped zinc telluro-fluoroborate glasses for laser and white LED applications." *Journal of Molecular Structure* 1125 (2016): 443-452. <https://doi.org/10.1016/j.molstruc.2016.06.080>
- [10] Şakar, Erdem, Özgür Fırat Özpolat, Bünyamin Alım, M. I. Sayyed, and Murat Kurudirek. "Phy-X/PSD: Development of a user friendly online software for calculation of parameters relevant to radiation shielding and dosimetry." *Radiation Physics and Chemistry* 166 (2020): 108496. <https://doi.org/10.1016/j.radphyschem.2019.108496>
- [11] Hassib, Mustafa Dh, Kawa M. Kaky, Ashok Kumar, Erdem Şakar, M. I. Sayyed, S. O. Baki, and M. A. Mahdi. "Boro-silicate glasses co-doped Er³⁺/Yb³⁺ for optical amplifier and gamma radiation shielding applications." *Physica B: Condensed Matter* 567 (2019): 37-44. <https://doi.org/10.1016/j.physb.2019.05.006>
- [12] Chanthima, N., J. Kaewkhao, P. Limkitjaroenporn, S. Tuscharoen, S. Kothan, M. Tungjai, S. Kaewjaeng, S. Sarachai, and P. Limsuwan. "Development of BaO-ZnO-B₂O₃ glasses as a radiation shielding material." *Radiation Physics and Chemistry* 137 (2017): 72-77. <https://doi.org/10.1016/j.radphyschem.2016.03.015>
- [13] Lakshminarayana, G., M. I. Sayyed, S. O. Baki, A. Lira, M. G. Dong, Kh A. Bashar, I. V. Kityk, and M. A. Mahdi. "Borotellurite glasses for gamma-ray shielding: an exploration of photon attenuation coefficients and structural and thermal properties." *Journal of Electronic Materials* 48 (2019): 930-941. <https://doi.org/10.1007/s11664-018-6810-8>
- [14] Aloraini, Dalal Abdullah, M. I. Sayyed, Aljawhara AH Almuqrin, Ashok Kumar, Thair Hussein Khazaalah, Sabina Yasmin, Mayeen Uddin Khandaker, and S. O. Baki. "Preparation, radiation shielding and mechanical characterization of PbO-TeO₂-MgO-Na₂O-B₂O₃ glasses." *Radiation Physics and Chemistry* 198 (2022): 110254. <https://doi.org/10.1016/j.radphyschem.2022.110254>
- [15] Abbas, Bashar Khudhair, Sharudin Omar Baki, Fong Wai Leng, Haider Khudhair Abbas, Layth Al-Sarraj, and Mohd Adzir Mahdi. "Investigation of structural, thermal properties and shielding parameters of borosilicate glasses doped with Dy³⁺/Tb³⁺ ions for gamma and neutron radiation shielding applications." *Journal of Advanced Research in Fluid Mechanics and Thermal Sciences* 80, no. 1 (2021): 50-61. <https://doi.org/10.37934/arfmts.80.1.5061>
- [16] Kaky, Kawa M., M. I. Sayyed, Farah Laariedh, Alyaa H. Abdalsalam, H. O. Tekin, and S. O. Baki. "Structural, optical and radiation shielding properties of zinc boro-tellurite alumina glasses." *Applied Physics A* 125 (2019): 1-12. <https://doi.org/10.1007/s00339-018-2329-3>
- [17] Sayyed, M. I., M. H. A. Mhareb, Betül Ceviz Şakar, K. A. Mahmoud, Erdem Şakar, Hammam Abdurabu Thabit, Kawa M. Kaky, and S. O. Baki. "Experimental investigation of structural and radiation shielding features of Li₂O-BaO-ZnO-B₂O₃-Bi₂O₃ glass systems." *Radiation Physics and Chemistry* 218 (2024): 111640. <https://doi.org/10.1016/j.radphyschem.2024.111640>
- [18] Divina, R., G. Sathiyapriya, K. Marimuthu, A. Askin, and M. I. Sayyed. "Structural, elastic, optical and γ-ray shielding behavior of Dy³⁺ ions doped heavy metal incorporated borate glasses." *Journal of Non-Crystalline Solids* 545 (2020): 120269. <https://doi.org/10.1016/j.jnoncrysol.2020.120269>
- [19] Rajaramakrishna, R., W. Chaiphaksa, S. Kaewjaeng, S. Kothan, and J. Kaewkhao. "Study of radiation shielding and luminescence properties of 1.5 μm emission from Er³⁺ doped zinc yttrium borate glasses." *Optik* 289 (2023): 171273. <https://doi.org/10.1016/j.ijleo.2023.171273>
- [20] Sayyed, M. I., and G. Lakshminarayana. "Structural, thermal, optical features and shielding parameters investigations of optical glasses for gamma radiation shielding and defense applications." *Journal of Non-Crystalline Solids* 487 (2018): 53-59. <https://doi.org/10.1016/j.jnoncrysol.2018.02.014>